

OF THE MAY 7, 1986 ANDREANOF ISLANDS EARTHQUAKE SOURCE PARAMETERS

Lorraine J. Hwang and Hiroo Kanamori

Seismological Laboratory, California Institute of Technology, Pasadena, CA 91125

Abstract. Source characteristics of the May 7, 1986 Andreanof Islands earthquake (51.412°N , 174.830°W , NEIC) are investigated from WWSSN, GDSN and IDA records. First motions from over 60 stations determine one steeply dipping nodal plane. We constrained this nodal plane and inverted long-period surface waves at a period of $T=256$ sec and determined the second nodal plane to be dip 18° , rake 116° , and strike 257° . This shallowly dipping thrust mechanism is consistent with plate motions in this region. Seismic moment from surface-wave inversion is 1.3×10^{28} dyne-cm corresponding to $M_w=8.0$. Amplitudes of body and surface waves from short-period instruments yield magnitudes of $m_b=6.8$ and $M_s=7.7$. The teleseismic average P-wave moment rate spectrum from 17 short- and intermediate-period instruments is slightly lower than that of an average $M_w=8.0$ subduction-zone event. We constrained the fault plane as determined above to deconvolve the first 90 secs of the long-period body wave at 11 teleseismic stations to determine the source time function and the spatial distribution of moment release. The source time function consists of 4 moment-releasing episodes which have a total moment release of 9.4×10^{27} dyne-cm. The fault ruptured bilaterally with the largest moment releasing subevent occurring between 30-45 sec. This subevent nucleates approximately 75-90 km west of the determined epicenter. This region corresponds to the epicentral area of the 1957 Great Aleutian earthquake which is one of the largest earthquakes in recorded history.

Introduction

The May 7, 1986 Andreanof Islands earthquake (22h 47m 10.2s UTC, 51.412°N , 174.830°W , $h=33$ km, $M_s=7.7$, NEIC) is the largest event that has occurred in this portion of the Aleutian arc since the 1957 Great Aleutian earthquake. The earthquake was felt on Atka approximately 65 km north of the epicenter and on Adak 130 km northwest and caused damage on both islands but no fatalities (Figure 1).

The Aleutian arc is one of the most seismically active regions in the world, and has generated several of the largest earthquakes in recorded history. These large earthquakes are a part of an earthquake sequence that ruptured most of the Alaska-Aleutian arc during the period 1938 to 1965. Areas that did not rupture during this period of increased activity have been identified as seismic gaps. These seismic gaps, the Yakataga, Shumagin, Unalaska and Kommandorski gaps have not broken in at least 80 yrs. Recurrence times of great earthquakes in this region

average about 80 yrs [Jacob, 1984]. However, they are estimated to be as low as 50 yrs and may exceed 100 yrs [Sykes, et. al, 1981].

The March 9, 1957 Great Aleutian earthquake, $M_w=9.1$, located at 51.3°N , 175.8°W , is one of the largest earthquakes in recorded history and occurred very close to this recent event. This earthquake ruptured a 1200 km segment of the arc. The aftershock sequence defines two segments of the rupture zone - one west of Amukta Pass (172°W) and one east [Mogi, 1968]. Since the arc ruptured here just 29 years ago, seismic potential in this area has been rated very low [Sykes, 1971; McCann, et. al, 1979; Sykes, et. al, 1981; Jacob, 1984].

The 1986 Andreanof Island earthquake occurred within the western aftershock zone of the 1957 Great Aleutian earthquake. Portions of the western aftershock zone have ruptured before in major events. Kisslinger [1985] examined the seismicity in a region between $175-178.8^\circ\text{W}$ called the Adak Seismic Zone. This zone ruptured in a sequence of large earthquakes ($M_s=7.8$) between 1901-1905 and in 1957. No great earthquakes have occurred in this region until 1986. The 1986 earthquake is unique because of the unexpectedly short recurrence time and the partial overlap of its rupture zone with the 1957 earthquake. To better understand this earthquake and its relationship to the 1957 earthquake, we examine the source characteristics of the May 7, 1986 earthquake over a broad period range (1-256 sec).

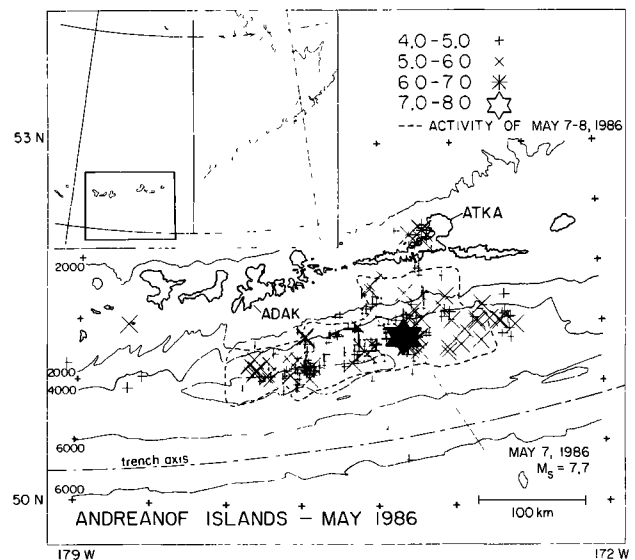


Figure 1. Map of a portion of the Aleutian Islands showing earthquake activity during May 1986 from the PDE catalog. The May 7, 1986 earthquake is plotted as a filled star. The aftershock area within 24 hrs following the main event is outlined in dashed lines.

Copyright 1986 by the American Geophysical Union.

Paper number 6L7064.
0094-8276/86/006L-7064\$03.00

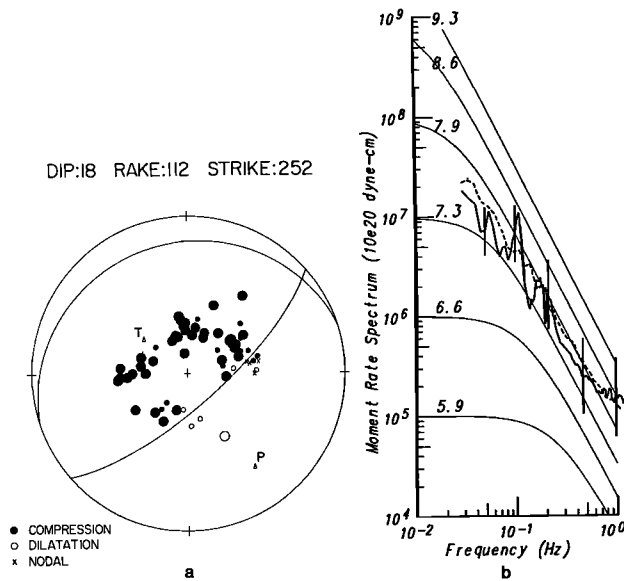


Figure 2. (a) Focal mechanism for the May 7, 1986 earthquake. Sixty-seven stations are used to constrain the steeply dipping nodal plane. Large symbols are good quality picks and small symbols poor quality. (b) Average moment rate spectra for the May 7, 1986 earthquake. Theoretical spectra for an ω^{-2} model are shown by thin lines. The dashed line shows the average spectrum from 7 events for an $M_w=8.0$ subduction zone event.

Aftershock Area

The 1986 Andreanof Islands earthquake was preceded by several foreshocks, the largest, $M_s=6.0$, occurring a little over two hours before the main event. Numerous aftershocks followed over the next several days (Figure 1). The aftershock area extends over a 220 km segment of the arc. The western extent of the aftershock zone is bounded by Adak Canyon. The eastern extent coincides with the eastern edge of the western aftershock zone of the 1957 event, strengthening the argument for a structural discontinuity (or barrier) here as proposed by Mogi [1968]. The aftershock zone grew northward toward Atka within the following weeks (Figure 1). Ensuing activity has been primarily restricted to within the above aftershock zone.

Kisslinger [1985] forecasted an earthquake measuring $M_s \geq 7$ to occur in late 1985 in the immediate vicinity of Adak Island and to rupture soon after into Adak Canyon. The epicentral region of this predicted event is over 150 km from the epicenter of the 1986 earthquake. Although the immediate aftershock sequence extends into the Adak Seismic Zone, it did not break into the Adak Canyon sub-region.

Focal Mechanism

The focal mechanism for the main event was determined from 67 World-Wide Standardized Seismograph Network (WWSSN) and Global Digital Seismograph Network (GDSN) stations. The first-motion data fix one of the nodal planes reasonably well (Figure 2a). Inversion of long-period surface waves

(described below) determined the second nodal plane to be dip 18° , rake 116° and strike 257° . This thrust mechanism is consistent with the orientation of the plate boundary and direction of plate motion in this region [Minster and Jordan, 1978].

Seismic Moment and Rupture Area

Seismic moment, M_0 , is determined from long-period surface waves from International Deployment of Accelerometers Network and GDSN stations following Kanamori and Given [1981]. Amplitude and phase spectral data at 256 sec are inverted using excitation functions for a source depth of 16 km. Since the source depth is less than 30 km, two elements of the seismic moment tensor cannot be resolved. We therefore use a double-couple source constraining one plane from the first-motion data. The source time delay is varied from 10 to 80 sec. Using 48 Rayleigh waves, R2-R4, the best fitting solution occurs at a source time delay of 60 sec which yields $M_0=1.3 \times 10^{28}$ dyne-cm, $M_w=8.0$. Adding 12 Love waves, G2-G4, gives approximately the same seismic moment. Since this is a very large event, directivity of the propagating dislocation causes the source time delay to be azimuthally dependent. Assuming a simple rupture propagating a distance of 150 km to the west at 3 km/sec and considering azimuth to the receiver, delay times are computed at each station. Using these times in the inversion does not significantly alter the solution. For simplicity, here we use a constant source delay time of 60 sec.

The aftershock data within the first 24 hrs of the mainshock suggest an immediate rupture zone of approximately 220 km in length and 65 km in width. Assuming rigidity is $\mu=5 \times 10^{11}$ dyne-cm $^{-2}$, the estimated slip during this event is 180 cm corresponding to a slip rate of 6.3 cm/yr since 1957. This estimate is somewhat lower than the average plate motion calculated by Minster and Jordan [1978]. The Minster and Jordan [1978] slip rate, 8.1 cm/yr, indicates a deficiency of slip of approximately 53 cm. This deficiency can be substantially reduced if aseismic slip is occurring (1.8 cm/yr) or rigidity of the fault plane surface is closer to crustal values.

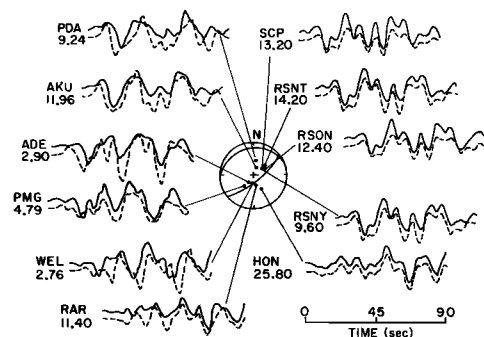


Figure 3. Comparison of actual (solid lines) and synthetic (dashed lines) seismograms from body wave inversion. Peak amplitudes for the data in cm is given below each station for a long period WWSSN instrument with a magnification of 1500. The focal mechanism and stations used in the inversion are shown.

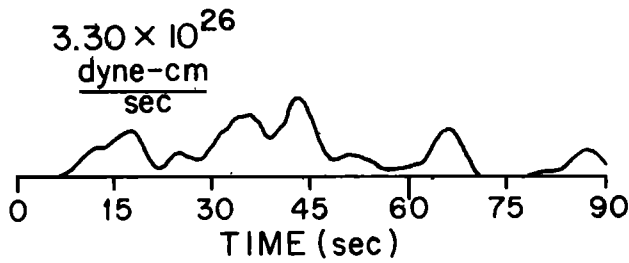


Figure 4. Source time function from the simultaneous body wave deconvolution. Peak moment release rate is 3.30×10^{26} dyne-cm/sec.

Magnitude and Source Spectra

Amplitudes of body and surface waves from short-period vertical component WWSSN and GDSN instruments yield a magnitude from Houston and Kanamori [1986] of $\hat{m}_b=6.8$ (40 station average) and an $M_s=7.7$ (33 station average) with a standard deviation of

$\sigma=0.34$ and $\sigma=0.32$ respectively. The average moment rate spectrum computed from 17 teleseismic P-wave seismograms from short- and intermediate-period vertical component GDSN instruments using the method of Houston and Kanamori [1986] is slightly lower than the average $M_w=8.0$ subduction-zone event (Figure 2b).

Rupture Pattern

The source time function is determined by simultaneous inversion of the first 90 sec of the body wave from 6 long-period WWSSN and 5 intermediate-period GDSN vertical component instruments following Kikuchi and Fukao [1985]. We use the focal mechanism as determined by the surface-wave inversion and extend the fault-plane surface discussed above from the aftershock data up to the trench axis. Figure 3 shows the best fitting synthetics compared to the data. The source time function for these synthetics is shown in Figure 4. For all models considered, the

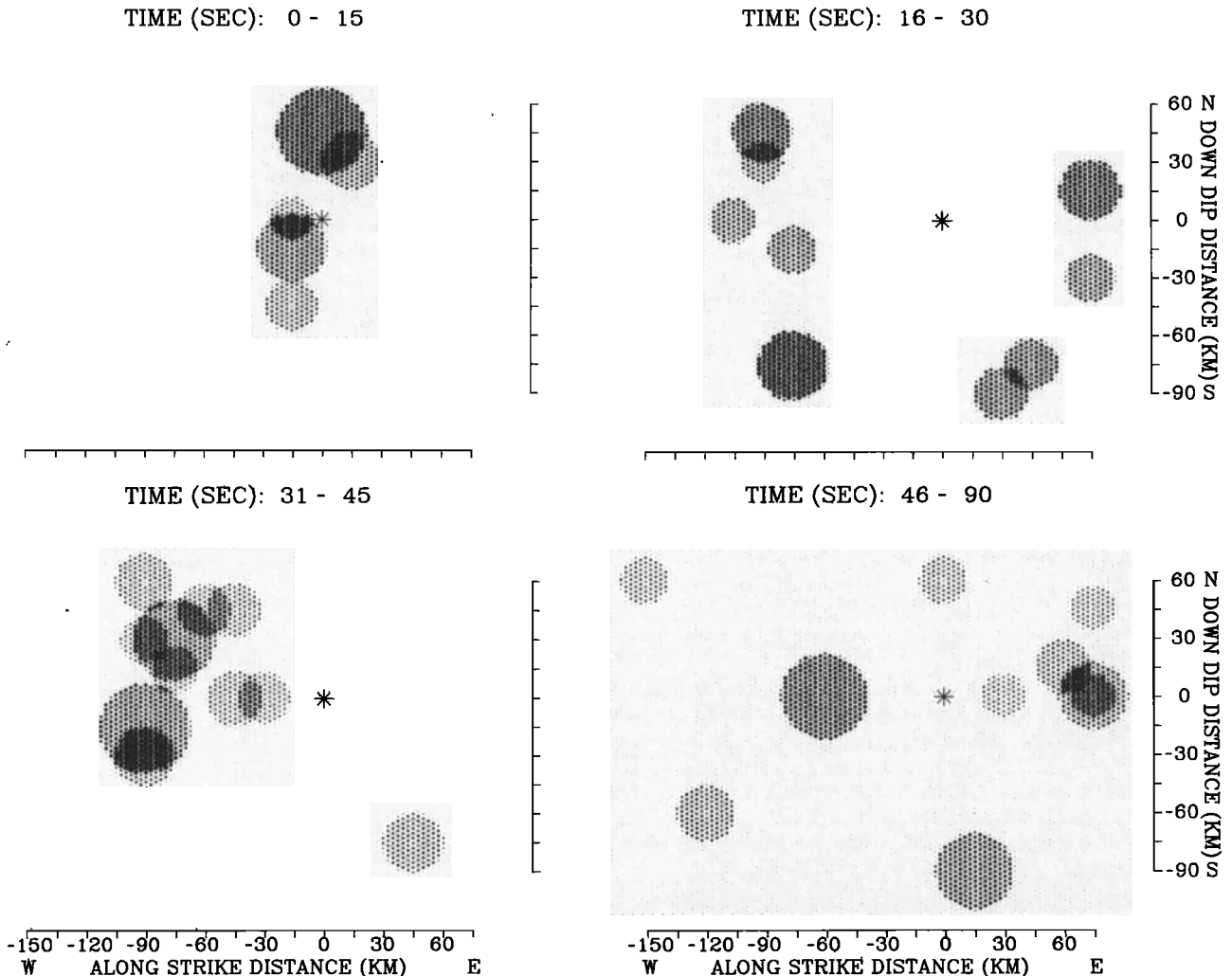


Figure 5. Fifteen second time slices of the spatial distribution of moment release projected onto the fault surface. The radius of each circle is proportional to the seismic moment of the point source it represents. Shading is proportional to the amount of moment release in a given area and is normalized to the maximum value in each time slice. The asterisk marks the hypocenter.

general features of the source time function are stable. The first moment-releasing episode is of lower amplitude and duration than the second and largest episode. Moment release then falls off with several smaller episodes occurring in the remaining 45 sec. Total moment release for this model is $M_0=9.4 \times 10^{27}$ dyne-cm.

With our distribution of stations, the rupture pattern (Figure 5) is resolved better along strike than perpendicular to strike. The first subevent occurs near the epicenter. The rupture area expands and moment release culminates in the second subevent between 30-45 sec. During this largest subevent, the point sources cluster about 75-90 km west of the epicenter. Remaining activity is diffuse.

The areas of the first two major subevents can be thought of as asperities along the fault surface. The first area is associated with the initial failure of the fault surface which perhaps triggered the failure of the second. Within the resolution of the data, the second and largest subevent corresponds to the epicenter of the 1957 earthquake.

Conclusion

The 1986 Andreanof Islands earthquake is the largest event to occur within the Islands since 1957. This great event, $M_0=1.3 \times 10^{28}$ dyne-cm, $M_w=8.0$, ruptured only 20% of the arc which failed in 1957. The end points of the aftershock region are well defined by Adak Canyon to the west and the eastern terminus of the western aftershock zone of 1957 to the east. Body wave modeling shows that this region is composed of 2 strong asperities, one which is associated with the 1986 epicenter and the other with the 1957 epicenter. The effect of rupturing of these two asperities within such a small portion of the 1957 aftershock zone is unclear. Li and Kisslinger [1984/85] find that rupture in adjacent fault segments can accelerate the loading rate and cause a coseismic stress jump in neighboring segments. This possibly triggers rupture of neighboring segments if it is at a high stress state. Hence, failure of adjacent segments due to accelerated loading from the 1986 earthquake depends on several poorly constrained parameters: current stress state, loading rates, and failure strengths. Further modeling of both stress transfer along plate boundaries and possible accelerated plate motions following great earthquakes [Anderson, 1985; Lyzenga, et al, 1986] must be considered to further understand plate interaction and seismic hazard in this region.

Acknowledgement. We thank the personnel from the WWSSN stations, Project IDA at the Institute for Geophysics and Planetary Physics at University of California, San Diego and the U.S. Geological Survey for making their data available to us. H. Houston helped us with the computation of the source spectra. Thoughtful reviews by L. Astiz and H. Houston were greatly appreciated. This research was supported by USGS Grant No. 14-08-0001-G1170 and partially by an NSF Graduate Fellowship. Contribution No. 4407,

Division of Geological and Planetary Sciences, California Institute of Technology, Pasadena, CA 91125.

References

- Anderson, D.L., Accelerated plate tectonics, *Science*, **187**, 1077-1079, 1985.
- Houston, H. and H. Kanamori, Source spectra of great earthquakes: teleseismic constraints on rupture process and strong motion, *Bull. Seism. Soc. Am.*, **76**, 19-42, 1986.
- Jacob, K.H., Estimates of long-term probabilities for great earthquakes in the Aleutians, *Geophys. Res. Lett.*, **11**, 295-298, 1984.
- Kanamori, H. and J.W. Given, Use of long-period surface waves for rapid determination of earthquake source parameters, *Phys. Earth Planet. Inter.*, **27**, 8-31, 1981.
- Kikuchi, M. and Y. Fukao, Iterative deconvolution of complex body waves from great earthquakes - the Tokachi-Oki earthquake of 1968, *Phys. Earth. Planet. Inter.*, **37**, 235-248, 1985.
- Kisslinger, C., Seismicity patterns in the Adak Seismic Zone and the short term outlook for a major earthquake, in *Minutes of the National Earthquake Prediction Council, September 8 & 9, Anchorage, Alaska*, edited by C.F. Shearer, U.S. Geological Survey Open File Report, 86-92, 120-134, 1985.
- Li, V.C. and C. Kisslinger, Stress transfer and non-linear stress accumulation of subduction-type plate boundaries - applications to the Aleutians, *Pure Appl. Geophys.*, **122**, 812-830, 1984/85.
- Lyzenga, G.A., A. Raefsky and B.H. Hager, Time-predictable earthquake recurrence at subduction zones? (abstract), *EOS Trans. AGU*, in press, 1986.
- McCann, W.R., S.P. Nishenko, L.R. Sykes and J. Krause, Seismic gaps and plate tectonics: Seismic potential for major plate boundaries, *Pure Appl. Geophys.*, **117**, 1082-1147, 1979.
- Minster, J.B. and T.H. Jordan, Present-day plate motions, *J. Geophys. Res.*, **83**, 5331-5354, 1978.
- Mogi, K., Development of aftershock areas of great earthquakes, *Bull. Earthquake Res. Inst. Tokyo Univ.*, **46**, 175-203, 1968.
- Sykes, L.R., Aftershock zones of great earthquakes, seismicity gaps, and earthquake prediction for Alaska and the Aleutians, *J. Geophys. Res.*, **76**, 8021-8041, 1971.
- Sykes, L.R., J.B. Kisslinger, L. House, J.N. Davies and K.H. Jacob, Rupture zones and repeat times of great earthquakes along the Alaska-Aleutian arc, 1784-1980, in *Earthquake Prediction, An International Review, Maurice Ewing Series, 4*, edited by D.W. Simpson and P.G. Richards, pp. 73-80, 1981.

(Received October 6, 1986;
accepted October 22, 1986.)